

NASA TECHNICAL NOTE



NASA TN D-6155

C.1

NASA TN D-6155

LOAN COPY: RETURN
AFWL (DOGL)
KIRTLAND AFB, N

0130045



TECH LIBRARY KAFB, NM

CALCULATED PRESSURE-INDUCED
VIBRATIONAL ABSORPTION
IN $H_2 - H_2$ COLLISIONS
IN HYDROGEN GAS

by R. W. Patch

*Lewis Research Center
Cleveland, Ohio 44135*



0133045

1. Report No. NASA TN D-6155	2. Government Accession No.	3. Recipient's Catalog No.	
4. Title and Subtitle CALCULATED PRESSURE-INDUCED VIBRATIONAL ABSORPTION IN H ₂ - H ₂ COLLISIONS IN HYDROGEN GAS	5. Report Date February 1971		6. Performing Organization Code
	7. Author(s) R. W. Patch		8. Performing Organization Report No. E-5843
9. Performing Organization Name and Address Lewis Research Center National Aeronautics and Space Administration Cleveland, Ohio 44135	10. Work Unit No. 122-28		11. Contract or Grant No.
	12. Sponsoring Agency Name and Address National Aeronautics and Space Administration Washington, D. C. 20546		13. Type of Report and Period Covered Technical Note
15. Supplementary Notes		14. Sponsoring Agency Code	
16. Abstract The coefficient for pressure-induced vibrational absorption in H ₂ - H ₂ collisions was calculated for temperatures from 298 to 7000 K and wave numbers between 100 and 40 000 cm ⁻¹ for transitions with a net change of +1 vibrational quanta. The absorption occurs principally in the infrared. The model included many refinements. The integrated absorption coefficient at 298 K was 87 percent of the experimental value. The integrated absorption coefficient at 3000 K was 2.1 times the previous theoretical value. For pressures from 100 to 1000 atm (1.013×10 ⁷ to 1.013×10 ⁸ N/m ²) the Planck and Rosseland mean opacities were increased by factors as high as 18.9 and 303, respectively, over previous estimates. An approximate formula for the spectral absorption coefficient is given for rapid calculation for temperatures from 600 to 7000 K.			
17. Key Words (Suggested by Author(s)) Hydrogen Pressure-induced absorption Vibrational absorption Absorption coefficient Opacity		18. Distribution Statement Unclassified - unlimited	
19. Security Classif. (of this report) Unclassified	20. Security Classif. (of this page) Unclassified	21. No. of Pages 41	22. Price* \$3.00

CALCULATED PRESSURE-INDUCED VIBRATIONAL ABSORPTION

IN $H_2 - H_2$ COLLISIONS IN HYDROGEN GAS

by R. W. Patch

Lewis Research Center

SUMMARY

The coefficient for pressure-induced vibrational absorption in $H_2 - H_2$ collisions was calculated for temperatures from 298 to 7000 K and wave numbers between 100 and 40 000 reciprocal centimeters for local thermodynamic equilibrium. Because only transitions with a net change of +1 vibrational quanta were considered, the absorption was centered near the fundamental at 4161 reciprocal centimeters in the infrared. The model included electronic configuration interaction, mechanical anharmonicity, vibration-rotation interaction, excited vibrational states, and more realistic intermolecular potential and line shapes than previously used. The integrated absorption coefficient at 298 K was 87 percent of the experimental value. The integrated absorption coefficient at 3000 K was 2.1 times the previous theoretical value. For pressures from 100 to 1000 atmospheres (1.013×10^7 to 1.013×10^8 N/m²) the Planck and Rosseland mean opacities were increased by factors as high as 18.9 and 303, respectively, over previous estimates. An approximate formula for the spectral absorption coefficient is given for rapid calculation for temperatures from 600 to 7000 K.

INTRODUCTION

The need for reliable heat-transfer calculations for high-temperature high-pressure hydrogen gas occurs in gaseous-core nuclear rockets (refs. 1 and 2), in outer layers of late-type stars, and in high-speed entry of spacecraft into certain planetary atmospheres. Such calculations require accurate pressure-induced vibrational absorption coefficients for $H_2 - H_2$ collisions. This absorption occurs in the infrared region and is principally due to transitions with a net change of +1 vibrational quanta for the two molecules. The special case where the vibrational quantum number of one molecule jumps from 0 to 1 is known as fundamental vibrational absorption.

Considerable theoretical work has been performed on pressure-induced $H_2 - H_2$ fundamental vibrational absorption. Isolated H_2 molecules do not possess an electric dipole moment, but a necessary condition for pressure-induced vibrational absorption is an electric dipole moment. This moment is induced during collisions. Van Kranendonk and Bird (ref. 3) gave a theory which assumed that the induced dipole moment was the sum of a contribution due to the overlap of orbitals and a contribution due to the electric quadrupole moment of each molecule inducing a dipole moment in the other molecule. This is called the large-R approximation in this report. They evaluated the overlap contribution by a distorted-orbital method. Britton and Crawford (ref. 4) improved Van Kranendonk and Bird's theory by including components of the dipole moment perpendicular to the intermolecular axis and by including an additional exchange effect in calculating the overlap dipole moment. Van Kranendonk (refs. 5 and 6) extended his theory to cryogenic temperatures by considering quantum effects in the translational motion of the gas molecules. Linsky (ref. 7) extrapolated Van Kranendonk's (ref. 6) theory to temperatures up to 3000 K although the theory neglected excited vibrational states. All theories have assumed a Lennard-Jones 6-12 intermolecular potential (ref. 8).

A great deal of experimental work has also been performed on pressure-induced $H_2 - H_2$ fundamental vibrational absorption. Experimental measurements of absorption coefficients have been made at temperatures up to 423 K (refs. 9 to 11) and are in general agreement with each other and with theory (refs. 4 and 6).

At temperatures several times higher than existing experimental data, several effects can be expected to be important that were not important in the experiments or theories. Excited vibrational states may be more important than their relative populations would indicate, and mechanical anharmonicity and vibration-rotation interaction should also have appreciable effects. In addition, as temperature is raised, collisions become harder so that induced dipole moment and intermolecular potential must be known for smaller intermolecular distances. It is not safe to extrapolate dipole moment from values for intermolecular distances important at room temperature because electronic configuration interaction is important at small intermolecular distances but not at large intermolecular distances. It is well known not to be safe to use a Lennard-Jones 6-12 intermolecular potential at high temperature because it gives excessive potentials for small intermolecular distances. Lastly, at high temperature the absorption coefficient must be reduced because of the effect of stimulated emission, which follows Kirchhoff's law. This has not been done correctly in some previous theories.

The object of this report was to calculate more realistic values of absorption coefficient for transitions with a net change of +1 vibrational quanta for temperatures up to 7000 K. All the above high-temperature effects were included as realistically as currently possible. The induced dipole moment was obtained from orthogonalized valence-bond configuration-interaction calculations for small intermolecular distances (ref. 12)

and by the large-R approximation for large intermolecular distances (ref. 13). The effects of excited vibrational states, mechanical anharmonicity, and vibration-rotation interaction were based on a new analysis presented in this report. (Configuration interaction, excited vibrational states, mechanically anharmonicity, and vibration-rotation interaction were not included in previous pressure-induced absorption theories.) More recent line shapes were used than Linsky (ref. 7) used. The temperature range 298 to 7000 K was covered. At higher temperatures other processes are much more important. This report is limited to densities where ternary collisions are not important (ref. 10).

ANALYSIS

In this section the integrated absorption coefficient is obtained for pressure-induced vibrational transitions including the effects of excited vibrational states, mechanical anharmonicity, and vibration-rotation interaction. The relation of this coefficient to several other absorption coefficients is then given, and realistic line shapes are selected based on experiments in the literature and on theoretical considerations.

Absorption Coefficients in Terms of Einstein Coefficients

The first step in getting the integrated absorption coefficient in useful form is to relate the linear absorption coefficient, the Einstein coefficients for absorption, and the integrated absorption coefficient. Consider a gas containing only H_2 molecules. We are interested in the pressure-induced vibrational absorption occurring during binary collisions of pairs of these molecules. Let v_i , J_i , and m_i be the vibrational quantum number, total angular momentum quantum number, and quantum number for the component of total angular momentum along the intermolecular axis, respectively, for the i^{th} molecule. (Symbols are given in the appendix.) A state ρ of the pair thus has the quantum numbers v_1 , v_2 , J_1 , J_2 , m_1 , and m_2 provided the molecules are far enough apart. We define a spectral Einstein coefficient of absorption $B_{\rho\rho'\tilde{\nu}}$ in such a way that the probability of a pair of molecules in state ρ , exposed to radiation of wave number $\tilde{\nu}$, absorbing a quantum $hc\tilde{\nu}$ in time interval dt and wave number interval $d\tilde{\nu}$ and making a transition to state ρ' is given by $B_{\rho\rho'\tilde{\nu}}\rho_{\tilde{\nu}} dt d\tilde{\nu}$, where $\rho_{\tilde{\nu}}$ is the radiation energy density per unit wave number.

According to Chandrasekhar (ref. 14), the linear absorption coefficient $a_{\tilde{\nu}}$ (excluding stimulated emission) is related to the spectral Einstein coefficient by

$$a_{\tilde{\nu}} = p_{\rho} B_{\rho\rho'\tilde{\nu}} \frac{h\tilde{\nu}}{V} \quad (1)$$

where V is the volume of homogeneous gas considered, p_ρ is the number of pairs in state ρ , and h is Planck's constant. The integrated Einstein coefficient of absorption for the transition $\rho \rightarrow \rho'$ is

$$B_{\rho\rho'} = \int_0^\infty B_{\rho\rho',\tilde{\nu}} d\tilde{\nu} \quad (2)$$

The integrated absorption coefficient with the wave number removed is defined by

$$s_{\rho\rho'} \equiv \int_0^\infty \frac{a_{\tilde{\nu}}}{\tilde{\nu}} d\tilde{\nu} \quad (3)$$

Combining equations (1) to (3),

$$s_{\rho\rho'} = \frac{p_\rho h B_{\rho\rho'}}{V} \quad (4)$$

However, $B_{\rho\rho'}$ actually depends on the intermolecular distance R of the pair of molecules (fig. 1), so equation (4) must be corrected by averaging over R . For a dilute system the averaging may be accomplished by (ref. 15)

$$s_{\rho\rho'} = \frac{p_\rho h}{V^2} \int_V B_{\rho\rho'} e^{-\Phi/kT} 4\pi R^2 dR \quad (5)$$

where Φ is the intermolecular potential averaged over orientations so that it depends only on R . For neutral molecules Φ decreases rapidly with increasing R , so the integration may be extended to $R = \infty$ without loss of accuracy.

More useful versions of equation (5) are obtained by replacing p_ρ by number densities and summing. The number of pairs of H_2 molecules is $N(N-1)/2$, where N is the number of such molecules in volume V . For $N \gg 1$ this is essentially $N^2/2$. The quantity p_ρ is thus

$$p_\rho = \binom{N^2}{2} P(v_1, J_1, m_1) P(v_2, J_2, m_2) \quad (6)$$

where $P(v, J, m)$ is the probability of an H_2 molecule having quantum numbers with values $v, J,$ and m . States with the same $v_1, v_2, J_1,$ and J_2 but any values of m_1 and m_2 all have the same energy. Likewise, states with the same $v_1', v_2', J_1',$ and J_2' but any values of m_1' and m_2' all have the same energy. Consequently, transitions between these primed and unprimed states all have the same wave number. Thus for convenience their integrated absorption coefficients (eq. (5)) may be added.

$$s_{\zeta\zeta'} = \frac{n^2 h}{2} \sum_{m_1=-J_1}^{J_1} \sum_{m_1'=-J_1'}^{J_1'} \sum_{m_2=-J_2}^{J_2} \sum_{m_2'=-J_2'}^{J_2'} P(v_1, J_1, m_1) P(v_2, J_2, m_2) \int_0^\infty B_{\rho\rho'} e^{-\Phi/kT} 4\pi R^2 dR \quad (7)$$

where subscript ζ stands for the quantum numbers $v_1, J_1, v_2,$ and J_2 ; a ρ prime indicates quantum numbers after the transition; and n is the number density corresponding to N .

Wave Functions and Expansions

The Einstein coefficient and hence $s_{\zeta\zeta'}$, may be expressed in terms of the wave functions and of expansion coefficients of the dipole moment. First a set of coordinates are needed. We neglect translation of the molecules and choose Cartesian coordinates fixed in space half way between the molecules (fig. 1).

The integrated Einstein coefficient is related to the components $(\mu_x)_{\rho'\rho}, (\mu_y)_{\rho'\rho},$ and $(\mu_z)_{\rho'\rho}$ of the electric dipole matrix elements for these coordinates by (ref. 16)

$$B_{\rho\rho'} = \frac{2\pi^2}{3h^2 \epsilon_0 c} \left[|(\mu_x)_{\rho'\rho}|^2 + |(\mu_y)_{\rho'\rho}|^2 + |(\mu_z)_{\rho'\rho}|^2 \right] \quad (8)$$

where ϵ_0 is the electric permittivity of free space, c is the velocity of light, and the equation is in SI units. The x and y contributions to equation (8) can be expected to be considerably smaller than the z contribution for two reasons: (1) The electric quadrupole moment of each molecule may induce a dipole in the other molecule. The average magnitudes of the x and y components of the electric fields due to these quadrupole

moments are much less than the z components. (2) The distortion of the orbitals due to overlap is principally in the z direction. Therefore the x and y contributions to equation (8) are neglected here. If equation (8) is substituted into equation (7), we get

$$S_{\xi\xi'} = \frac{\pi^2 n^2 P(v_1, J_1, 0) P(v_2, J_2, 0)}{3hc\epsilon_0} \int_0^\infty \sum_{m_1=-J_1}^{J_1} \sum_{m_1'=-J_1'}^{J_1'} \sum_{m_2=-J_2}^{J_2} \sum_{m_2'=-J_2'}^{J_2'} \times \left| \left(\mu_z \right)_{\rho'\rho} \right|^2 e^{-\Phi/kT} 4\pi R^2 dR \quad (9)$$

where the fact that $P(v, J, m)$ is independent of m has been used.

The relation between the matrix element $\left(\mu_z \right)_{\rho'\rho}$ and the system wave functions ψ_ρ and $\psi_{\rho'}$ is

$$\left(\mu_z \right)_{\rho'\rho} = \int \psi_{\rho'}^* \left(- \sum_i e z_i + \sum_j e Z_j z_j \right) \psi_\rho d\tau \quad (10)$$

where z_i is the z coordinate of the i^{th} electron, z_j is the z coordinate of the j^{th} nucleus, e is the charge of an electron, eZ_j is the charge of the j^{th} nucleus, and the summations cover all electrons and nuclei. If the relative motion of the two molecules is slow compared to the motion of the electrons, the Born-Oppenheimer approximation (ref. 17) may be applied to the pair of molecules collectively.

$$\psi_\rho = \psi_e(X_i, R, r_1, r_2, \theta_1, \varphi_1, \theta_2, \varphi_2) \psi_n(R, r_1, r_2, \theta_1, \varphi_1, \theta_2, \varphi_2) \quad (11)$$

where ψ_e is the electronic wave function, and ψ_n is the nuclear wave function. In equation (11) X_i stands for the position coordinates of the electrons, r_1 for the internuclear distance of molecule 1, and r_2 for the internuclear distance of molecule 2. It has been observed that the wave numbers of lines in pressure-induced transitions can be calculated from term values for isolated diatomic molecules. Consequently, it is reasonable to approximate ψ_n by (ref. 3)

$$\psi_n \approx \frac{\psi_{v_1 J_1}(r_1)}{r_1} \frac{\psi_{v_2 J_2}(r_2)}{r_2} Y_{J_1 m_1}(\theta_1, \varphi_1) Y_{J_2 m_2}(\theta_2, \varphi_2) \quad (12)$$

where ψ_{vJ} is the vibrational wave function. In the past harmonic oscillator wave functions have been used for ψ_{vJ} , but in this report mechanical anharmonicity is included by using a wave function calculated from the Rydberg-Klein-Rees potential energy for an isolated H_2 molecule. In addition, vibration-rotation interaction in H_2 is included by adding $h^2 J(J+1)/8\pi^2 m_r r^2$ to the potential energy (ref. 18) before calculating the vibrational wave function. In equation (12) Y_{Jm} is the spherical harmonic given by

$$Y_{Jm}(\theta, \varphi) = (2\pi)^{-1/2} \Theta_{Jm}(\cos \theta) e^{im\varphi} \quad (13)$$

For $m \geq 0$ the normalized associated Legendre functions Θ_{Jm} are given by Pauling and Wilson (ref. 19). For $m < 0$ they are

$$\Theta_{Jm}(\cos \theta) = (-1)^m \Theta_{J|m|}(\cos \theta) \quad (14)$$

From equations (10) to (12)

$$\begin{aligned} (\mu_z)_{\rho, \rho} = & \int_0^{2\pi} \int_0^\pi \int_0^{2\pi} \int_0^\pi \int_0^\infty \int_0^\infty \psi_{v_1 J_1}^* \psi_{v_2 J_2}^* Y_{J_1 m_1}^* Y_{J_2 m_2}^* \mu_z \\ & \times \psi_{v_1 J_1} \psi_{v_2 J_2} Y_{J_1 m_1} Y_{J_2 m_2} \sin \theta_1 \sin \theta_2 dr_1 dr_2 d\theta_1 d\varphi_1 d\theta_2 d\varphi_2 \end{aligned} \quad (15)$$

where the z component of the electric dipole moment is given by

$$\mu_z = \int \psi_e^* \left(- \sum_i e z_i + \sum_j e Z_j z_j \right) \psi_e d\tau_e \quad (16)$$

Because z_i is a linear, Hermitian operator, μ_z must be real. The dipole moment μ_z may be expanded in a Taylor series about the equilibrium internuclear distances r_1^0 and r_2^0 of the molecules.

$$\begin{aligned} \mu_z(R, r_1, r_2, \theta_1, \varphi_1, \theta_2, \varphi_2) = & \mu_z^0(R, \theta_1, \varphi_1, \theta_2, \varphi_2) + \mu_1(R, \theta_1, \varphi_1, \theta_2, \varphi_2)(r_1 - r_1^0) \\ & + \mu_2(R, \theta_1, \varphi_1, \theta_2, \varphi_2)(r_2 - r_2^0) \end{aligned} \quad (17)$$

where μ_z^0 is the value of u_z for r_1^0 and r_2^0 , μ_1 is $\partial\mu_z/\partial r_1$, and μ_2 is $\partial\mu_z/\partial r_2$, both evaluated for r_1^0 and r_2^0 . The quantities μ_z^0 and μ_1 can be expanded in spherical harmonics.

$$\mu_z^0(R, \theta_1, \varphi_1, \theta_2, \varphi_2) = \sum_{l_1=0}^{\infty} \sum_{\xi_1=-l_1}^{l_1} \sum_{l_2=0}^{\infty} \sum_{\xi_2=-l_2}^{l_2} 2\pi C_{l_1\xi_1 l_2\xi_2}^{(R)} \times Y_{l_1\xi_1}(\theta_1, \varphi_1) Y_{l_2\xi_2}(\theta_2, \varphi_2) \quad (18)$$

$$\mu_1(R, \theta_1, \varphi_1, \theta_2, \varphi_2) = \sum_{l_1=0}^{\infty} \sum_{\xi_1=-l_1}^{l_1} \sum_{l_2=0}^{\infty} \sum_{\xi_2=-l_2}^{l_2} 2\pi D_{l_1\xi_1 l_2\xi_2}^{(R)} \times Y_{l_1\xi_1}(\theta_1, \varphi_1) Y_{l_2\xi_2}(\theta_2, \varphi_2) \quad (19)$$

where $C_{l_1\xi_1 l_2\xi_2}$ and $D_{l_1\xi_1 l_2\xi_2}$ are expansion coefficients to be determined.

Molecular Symmetry and Configurations

Considerable simplification of equations (18) to (19) is possible. Some of the expansion coefficients are zero because of molecular symmetry. The operation

$$\varphi_i \rightarrow \varphi_i + \pi$$

$$\theta_i \rightarrow \pi - \theta_i$$

which is equivalent to interchanging the two identical nuclei, should not change μ_z^0 or μ_1 for $i = 1$ or 2 . In addition, μ_z^0 and μ_1 should have azimuthal dependence solely on $\varphi_2 - \varphi_1$ because the orientation of the x and y axes should have no effect. Thus, the only nonzero $C_{l_1\xi_1 l_2\xi_2}$ are C_{0000} , C_{2000} , C_{0020} , C_{2020} , C_{2-121} , C_{212-1} , C_{2-222} , C_{222-2} , and $C_{l_1\xi_1 l_2\xi_2}$ with $l_1 \geq 4$ or $l_2 \geq 4$. Also, $C_{2-121} = C_{212-1}$ because μ_z^0

must not depend on what direction about the z axis φ_1 and φ_2 are measured. Similarly $C_{2-222} = C_{222-2}$. All the preceding findings apply to the $D_{l_1\xi_1 l_2\xi_2}$ as well.

Further simplification of equations (18) to (19) is necessary because calculations of μ_z are time consuming even on a high-speed digital computer. This is especially true if small values of R are involved, which occurs at high temperature. Thus it is necessary to limit the number of configurations $\theta_1, \varphi_1, \theta_2, \varphi_2$ to as few as possible. The ones selected are shown in figure 2. The Θ_{21} and Θ_{2-1} are zero for all these configurations, so $C_{2-121}, C_{212-1}, D_{2-121}$, and D_{212-1} cannot be determined. There are just enough configurations to determine all remaining nonzero $C_{l_1\xi_1 l_2\xi_2}$ and $D_{l_1\xi_1 l_2\xi_2}$ with $l_1 < 4$ and $l_2 < 4$. Neglect of expansion coefficients with $l_1 \geq 4$ and/or $l_2 \geq 4$ is reasonable because, if such coefficients were nonzero they would allow transitions with J_1 or J_2 changing by ± 4 or more, which have never been observed. For $r_1 = r_1^0$ and $r_2 = r_2^0$, μ_z is zero for configurations 1, 2, and 5 by symmetry and differs only in sign for configurations 3 and 4. Hence equation (18) gives

$$\left. \begin{aligned} 0 &= \frac{1}{2} C_{0000} + \frac{\sqrt{5}}{2} C_{2000} + \frac{\sqrt{5}}{2} C_{0020} + \frac{5}{2} C_{2020} + OC_{2-222} \\ 0 &= \frac{1}{2} C_{0000} - \frac{\sqrt{5}}{4} C_{2000} - \frac{\sqrt{5}}{4} C_{0020} + \frac{5}{8} C_{2020} + \frac{15}{8} C_{2-222} \\ -\mu_{z,4}^0 &= \frac{1}{2} C_{0000} + \frac{\sqrt{5}}{2} C_{2000} - \frac{\sqrt{5}}{4} C_{0020} - \frac{5}{4} C_{2020} + OC_{2-222} \\ \mu_{z,4}^0 &= \frac{1}{2} C_{0000} - \frac{\sqrt{5}}{4} C_{2000} + \frac{\sqrt{5}}{2} C_{0020} - \frac{5}{4} C_{2020} + OC_{2-222} \\ 0 &= \frac{1}{2} C_{0000} - \frac{\sqrt{5}}{4} C_{2000} - \frac{\sqrt{5}}{4} C_{0020} + \frac{5}{8} C_{2020} - \frac{15}{8} C_{2-222} \end{aligned} \right\} \quad (20)$$

This has the solution $C_{0000} = C_{2020} = C_{2-222} = 0$, $C_{2000} = -C_{0020}$.

The derivative μ_2 can be expressed in terms of μ_1 . To do this, an arbitrary configuration is reflected in a plane bisecting the intermolecular axis, with the result

$$\mu_2(R, \theta_1, \varphi_1, \theta_2, \varphi_2) = -\mu_1(R, \pi - \theta_2, \varphi_2, \pi - \theta_1, \varphi_1) \quad (21)$$

where the order of the arguments of μ_1 has the significance given in equation (19). Substituting equation (21) into equation (17) gives

$$\begin{aligned} \mu_z = & \mu_z^0(\mathbf{R}, \theta_1, \varphi_1, \theta_2, \varphi_2) + \mu_1(\mathbf{R}, \theta_1, \varphi_1, \theta_2, \varphi_2)(r_1 - r^0) \\ & - \mu_1(\mathbf{R}, \pi - \theta_2, \varphi_2, \pi - \theta_1, \varphi_1)(r_2 - r^0) \end{aligned} \quad (22)$$

Evaluation of Integrals and Sums

The quadruple sum of the squares of the dipole matrix elements in equation (9) can be expressed simply in terms of vibrational overlap integrals, vibrational matrix elements, expansion coefficients, and Kronecker delta functions.

The first step is to combine equations (15), (18), (19), and (22) with the result

$$\begin{aligned} \left(\mu_z\right)_{\rho', \rho} = & M_1 A_{00}(1) A_{00}(2) + M_2 A_{20}(1) A_{00}(2) + M_3 A_{00}(1) A_{20}(2) + M_4 A_{20}(1) A_{20}(2) \\ & + M_5 A_{2-2}(1) A_{22}(2) + M_5 A_{22}(1) A_{2-2}(2) \end{aligned} \quad (23)$$

where

$$A_{ij}(\mathbf{k}) \equiv \delta(m'_k, j + m_k) \int_0^\pi \Theta_{J'_k m'_k} \Theta_{ij} \Theta_{J_k m_k} \sin \theta_k d\theta_k \quad (24)$$

$$M_1 \equiv (\Delta_1 Q_2 - Q_1 \Delta_2) D_{0000}$$

$$M_2 \equiv Q_1 Q_2 C_{2000} + \Delta_1 Q_2 D_{2000} - Q_1 \Delta_2 D_{0020}$$

$$M_3 \equiv -Q_1 Q_2 C_{2000} + \Delta_1 Q_2 D_{0020} - Q_1 \Delta_2 D_{2000}$$

$$M_4 \equiv (\Delta_1 Q_2 - Q_1 \Delta_2) D_{2020}$$

$$M_5 \equiv (\Delta_1 Q_2 - Q_1 \Delta_2) D_{2-222} \quad (25)$$

$$Q_k \equiv \int_0^\infty \psi_{v'_k J'_k}^* \psi_{v_k J_k} dr_k \quad (26)$$

$$\Delta_{\mathbf{k}} \equiv \int_0^\infty \psi_{v_{\mathbf{k}}' J_{\mathbf{k}}'}^*(r_{\mathbf{k}} - r^0) \psi_{v_{\mathbf{k}} J_{\mathbf{k}}} dr_{\mathbf{k}} \quad (27)$$

The quantities $Q_{\mathbf{k}}$ and $\Delta_{\mathbf{k}}$ are the vibrational overlap integral and vibrational matrix element, respectively. The quantity $\delta(m_{\mathbf{k}}', j + m_{\mathbf{k}})$ is the Kronecker delta function. The $A_{ij}(\mathbf{k})$ are readily evaluated by using the properties (ref. 20) and orthogonality of the normalized associated Legendre functions.

$$A_{00}(\mathbf{k}) = 2^{-1/2} \delta(m', m) \delta(J', J) \quad (28)$$

$$A_{20}(\mathbf{k}) = \frac{\sqrt{10}}{4} \left(3 \left\{ \frac{[(J+1)^2 - m^2][(J+2)^2 - m^2]}{(2J+1)(2J+3)^2(2J+5)} \right\}^{1/2} \delta(J', J+2) + \frac{2J(J+1) - 6m^2}{(2J+3)(2J-1)} \delta(J', J) \right. \\ \left. + 3 \left\{ \frac{[J^2 - m^2][(J-1)^2 - m^2]}{(2J+1)(2J-1)^2(2J-3)} \right\}^{1/2} \delta(J', J-2) \right) \delta(m', m) \quad (29)$$

$$A_{22}(\mathbf{k}) = \frac{\sqrt{15}}{4} \left\{ \left[\frac{(J+m+4)(J+m+3)(J+m+2)(J+m+1)}{(2J+5)(2J+3)^2(2J+1)} \right]^{1/2} \delta(J', J+2) \right. \\ \left. - 2 \left[\frac{(J+m+2)(J+m+1)(J-m)(J-m-1)}{(2J+3)^2(2J-1)^2} \right]^{1/2} \delta(J', J) \right. \\ \left. + \left[\frac{(J-m)(J-m-1)(J-m-2)(J-m-3)}{(2J+1)(2J-1)^2(2J-3)} \right]^{1/2} \delta(J', J-2) \right\} \delta(m', m+2) \quad (30)$$

$$\begin{aligned}
A_{2-2}^{(k)} = & \frac{\sqrt{15}}{4} \left\{ \left[\frac{(J-m+4)(J-m+3)(J-m+2)(J-m+1)}{(2J+5)(2J+3)^2(2J+1)} \right]^{1/2} \delta(J', J+2) \right. \\
& - 2 \left[\frac{(J-m+2)(J-m+1)(J+m)(J+m-1)}{(2J+3)^2(2J-1)^2} \right]^{1/2} \delta(J', J) \\
& \left. + \left[\frac{(J+m)(J+m-1)(J+m-2)(J+m-3)}{(2J+1)(2J-1)^2(2J-3)} \right]^{1/2} \delta(J', J-2) \right\} \delta(m', m-2) \quad (31)
\end{aligned}$$

where the subscript k is understood to apply to all quantities on the right sides of equations (28) to (31).

Squaring and summing equation (23) and making use of equations (28) to (31) gives

$$\begin{aligned}
\sum_{m_1=-J_1}^{J_1} \sum_{m_1'=-J_1'}^{J_1'} \sum_{m_2=-J_2}^{J_2} \sum_{m_2'=-J_2'}^{J_2'} \left| \left(\mu_z \right)_{\rho', \rho} \right|^2 = & M_1^2 L_0(J_1', J_1) L_0(J_2', J_2) \\
& + M_2^2 L_2(J_1', J_1) L_0(J_2', J_2) + M_3^2 L_0(J_1', J_1) L_2(J_2', J_2) \\
& + \left(M_4^2 + 2M_5^2 \right) L_2(J_1', J_1) L_2(J_2', J_2) \quad (32)
\end{aligned}$$

where

$$L_0(J', J) \equiv \left[\frac{(2J+1)}{2} \right] \delta(J', J) \quad (33)$$

$$\begin{aligned}
L_2(J', J) \equiv & \frac{3}{4} \frac{(J+1)(J+2)}{2J+3} \delta(J', J+2) + \frac{1}{2} \frac{(J+1)(2J+1)J}{(2J+3)(2J-1)} \delta(J', J) + \frac{3}{4} \frac{(J-1)J}{2J-1} \delta(J', J-2) \\
& \quad (34)
\end{aligned}$$

Final Integrated Absorption Coefficient and Relation

to Other Absorption Coefficients

The final equation for the integrated absorption coefficient $s_{\zeta\zeta'}$, is obtained by substituting equation (32) into equation (9)

$$s_{\zeta\zeta'} = \frac{\pi^2 n^2 P(v_1, J_1, 0) P(v_2, J_2, 0) W}{3hc\epsilon_0} \quad (35)$$

where

$$W \equiv L_0(J_1', J_1) L_0(J_2', J_2) G_1 + L_2(J_1', J_1) L_0(J_2', J_2) G_2 + L_0(J_1', J_1) L_2(J_2', J_2) G_3 \\ + L_2(J_1', J_1) L_2(J_2', J_2) G_{45} \quad (36)$$

$$G_1 \equiv (\Delta_1 Q_2 - Q_1 \Delta_2)^2 I_1 \quad (37)$$

$$G_2 \equiv Q_1^2 Q_2^2 I_6 + \Delta_1^2 Q_2^2 I_2 + Q_1^2 \Delta_2^2 I_3 + 2Q_1 \Delta_1 Q_2^2 I_7 - 2Q_1^2 Q_2 \Delta_2 I_8 - 2Q_1 \Delta_1 Q_2 \Delta_2 I_9 \quad (38)$$

$$G_3 \equiv Q_1^2 Q_2^2 I_6 + \Delta_1^2 Q_2^2 I_3 + Q_1^2 \Delta_2^2 I_2 - 2Q_1 \Delta_1 Q_2^2 I_8 + 2Q_1^2 Q_2 \Delta_2 I_7 - 2Q_1 \Delta_1 Q_2 \Delta_2 I_9 \quad (39)$$

$$G_{45} \equiv (\Delta_1 Q_2 - Q_1 \Delta_2)^2 (I_4 + 2I_5) \quad (40)$$

$$I_i = \int_0^\infty e^{-\Phi/kT} E_i(R) 4\pi R^2 dR \quad (i = 1, 9) \quad (41)$$

E_i is D_{0000}^2 , D_{2000}^2 , D_{0020}^2 , D_{2020}^2 , D_{2-222}^2 , C_{2000}^2 , $C_{2000} D_{2000}$, $C_{2000} D_{0020}$, and $D_{2000} D_{0020}$ for $i = 1$ to 9 , respectively.

In applying equations (35) to (41) there are several subtleties to note. There is no restriction on v_1 or v_2 , so excited vibrational states may be included. There is no restriction on which v changes or how much it changes. In fact, one or both may change in a transition. Also, there is no restriction on whether v_1 or v_2 increases or decreases provided that the wave number of the resulting transition is positive. Neither,

one or both J's may change, but the changes are limited to $J' - J = \pm 2$. If equation (35) is applied to a fundamental vibrational transition, the transitions with v_1 changing are considered distinct from those with v_2 changing.

The effects of mechanical anharmonicity and vibration-rotation interaction are contained in equations (35) to (41). Specifically, these effects influence the values of $P(v_1, J_1, 0)$, $P(v_2, J_2, 0)$, Q_1 , Q_2 , Δ_1 , and Δ_2 . The model used in deriving equations (35) to (41) is called the vibrating-rotator model for brevity.

The integrated absorption coefficient s of a transition with the wave number removed was defined by equation (3) but is density dependent. To remove this density dependence we define a new integrated absorption coefficient S for the $\zeta \rightarrow \zeta'$ transition.

$$S \equiv \frac{s_{\zeta\zeta'}}{\rho^2} \quad (42)$$

where ρ is dimensionless H_2 density given by

$$\rho \equiv \frac{n}{n_0} \quad (43)$$

and n_0 is the Loschmidt number. If $s_{\zeta\zeta'}$ is appropriately summed, equation (42) can be modified so S applies to a rotational branch or branches or to all transitions with a net change of +1 vibrational quanta.

The spectral absorption coefficient with the wave number removed is defined by

$$\tilde{A}_{\tilde{\nu}} \equiv \frac{a_{\tilde{\nu}}}{\rho^2} \quad (44)$$

Then

$$S = \int_0^{\infty} \tilde{A}_{\tilde{\nu}} d\tilde{\nu} \quad (45)$$

Assuming local thermodynamic equilibrium, the spectral absorption coefficient including wave number and stimulated emission is (ref. 21)

$$A_{\tilde{\nu}} = \tilde{A}_{\tilde{\nu}} \tilde{\nu} \left(1 - e^{-hc\tilde{\nu}/kT} \right) \quad (46)$$

so the attenuation of a monochromatic light beam by a path length l in H_2 gas is

$$\frac{I}{I_0} = e^{-A_{\tilde{\nu}} \rho^2 l} \quad (47)$$

Line Shapes

The line shape for a transition depends on what mechanism induces the electric dipole moment that makes the transition possible. For pressure-induced transitions there are two mechanisms: (1) the quadrupole moment of a molecule can induce a dipole moment in another molecule or (2) the overlap of the electron orbitals of two molecules can distort the orbitals and thereby cause a dipole moment. For fundamental vibrational transitions at room temperature and below, the principal mechanism has been found to depend on which rotational branch the transition belongs to (ref. 11). Only transitions in which the total angular momentum of not more than one molecule changes are important. Such transitions are classified into O, Q, or S branches according to whether J changes by -2 , 0 , or $+2$, respectively, in an absorption transition.

At room temperature the Q branch is principally due to the overlap dipole moment whereas the O and S branches are principally due to the quadrupole-induced dipole moment. Poll (ref. 21) has stated that line profiles in vibrational and rotational spectra which are due to the same quadrupole-induced effect have the same shapes, and those due to overlap effect have about the same shapes. At higher temperatures it is impossible to separate the quadrupole and overlap effects, so we assume one shape for all Q-branch lines and another shape for all O- and S-branch lines. The shapes are based primarily on experimental results. For both shapes

$$\tilde{A}_{\tilde{\nu}} = \frac{S f_{\tilde{\nu}}}{\int_0^{\infty} f_{\tilde{\nu}} d\tilde{\nu}} \quad (48)$$

where $f_{\tilde{\nu}}$ is the line shape function.

Q-branch lines. - From Hunt and Welsh (ref. 11)

$$f_{\tilde{\nu}} = \frac{w_Q^2 \exp\left(-hc \frac{\tilde{\nu}_0 - \tilde{\nu}}{kT}\right)}{(\tilde{\nu} - \tilde{\nu}_0)^2 + w_Q^2} \quad (\tilde{\nu} < \tilde{\nu}_0) \quad (49)$$

$$f_{\tilde{\nu}} = \frac{w_Q^2}{(\tilde{\nu} - \tilde{\nu}_0)^2 + w_Q^2} \quad (\tilde{\nu}_0 \leq \tilde{\nu}) \quad (50)$$

where $\tilde{\nu}_0$ is the wave number of the line computed from the term values, and w_Q is the half width given by

$$w_Q = 290 \left(\frac{T}{300^\circ \text{K}} \right)^{1/2} \text{ cm}^{-1} \quad (51)$$

Watanabe and Welsh (ref. 22) noted that for H_2 - He mixtures the high wave number wing was exponential for $(\tilde{\nu} - \tilde{\nu}_0)/w_Q > 0.7$. In addition, for theoretical reasons all moments of a line should be finite (private communication from V. F. Sears, Atomic Energy of Canada, Ltd., Chalk River, Ontario). This requirement is satisfied by an exponential tail but not by a dispersion tail. Hence we assume

$$f_{\tilde{\nu}} = F \exp \left(-U \frac{\tilde{\nu} - \tilde{\nu}_0}{w_Q} \right) \quad (\tilde{\nu}_0 + 0.7w_Q < \tilde{\nu} < \infty) \quad (52)$$

where F and U are constants chosen so equations (50) and (52) agree in value and slope for $\tilde{\nu} = \tilde{\nu}_0 + 0.7 w_Q$.

O- and S-branch lines. - From MacTaggart and Hunt (ref. 23) the shape of pure rotational lines of pure hydrogen is

$$f_{\tilde{\nu}} = \frac{w_S^2 \exp \left(-hc \frac{\tilde{\nu}_0 - \tilde{\nu}}{kT} \right)}{(\tilde{\nu} - \tilde{\nu}_0)^2 + w_S^2} \quad (\tilde{\nu} < \tilde{\nu}_0) \quad (53)$$

$$f_{\tilde{\nu}} = \frac{w_S^2}{(\tilde{\nu} - \tilde{\nu}_0)^2 + w_S^2} \quad (\tilde{\nu}_0 \leq \tilde{\nu} \leq \tilde{\nu}_0 + 1.73w_S) \quad (54)$$

$$f_{\tilde{\nu}} = \frac{M}{(\tilde{\nu} - \tilde{\nu}_0)^{2.40}} \quad (\tilde{\nu}_0 + 1.73w_S < \tilde{\nu} < \tilde{\nu}_0 + 7w_S) \quad (55)$$

where the line width is

$$w_S = 133 \left(\frac{T}{298^\circ\text{K}} \right)^{1/2} \text{ cm}^{-1} \quad (56)$$

and M was chosen so equations (54) to (55) have the same value at $\tilde{\nu} = \tilde{\nu}_O + 1.73w_S$. Because pure rotational lines are principally quadrupole induced, equations (53) to (56) can also be used for vibrational O and S lines. For the same reason as before, we assume an exponential tail.

$$f_{\tilde{\nu}} = G \exp \left(-H \frac{\tilde{\nu} - \tilde{\nu}_O}{w_S} \right) \quad (\tilde{\nu}_O + 7w_S < \tilde{\nu} < \infty) \quad (57)$$

where G and H are constants chosen so equations (55) and (57) agree in value and slope for $\tilde{\nu} = \tilde{\nu}_O + 7w_S$.

RESULTS AND DISCUSSION

Dipole Moment Integrals

Calculating the dipole moment integrals I_1 to I_9 requires the expansion coefficients of the dipole moment and its derivative and also the intermolecular potential. The major contributions to the dipole moment integrals come from $R = 2.5$ to 8 bohr (1.323×10^{-10} to 4.233×10^{-10} m) so reliable expansion coefficients and potential are required for this range.

Expansion coefficients were obtained by five methods, the method used depending on the value of R . Expansion coefficients for $R = 2.5$ to 4 bohr (1.323×10^{-10} to 2.117×10^{-10} m) were obtained by an orthogonalized valence-bond calculation including full configuration interaction (ref. 12). The results are given in table I. For $R = 6$ to 8 bohr (3.175×10^{-10} to 4.233×10^{-10} m) they were obtained by the large- R approximation (ref. 13). Both sets are shown in figures 3 and 4. For $R = 4$ to 6 bohr (2.117×10^{-10} to 3.175×10^{-10} m) the two sets were faired together by means of curves of the form: Coefficient = $c_1 R^{-4} + c_2 + c_3 R + c_4 R^2$, where c_1 to c_4 are constants. This is also shown in figures 3 and 4. For $R = 0$ all the expansion coefficients must be zero. Hence for $R = 0$ to 2.5 bohr (0 to 1.323×10^{-10} m) the expansion coefficients were interpolated. For $R > 8$ bohr (4.233×10^{-10} m) they were extrapolated.

The intermolecular potential was obtained by one method for large R and another

for small R . For $R \geq 4$ bohr (2.117×10^{-10} m) the Morse potential of Fisher (ref. 24) was used. Fisher fitted his potential to eight sets of experimental data (refs. 25 to 32). The viscosity data (refs. 25 to 31) were taken at temperatures between 200 and 2341 K. Second virial coefficient data (ref. 32) were also included by Fisher. For $R < 4$ bohr (2.117×10^{-10} m) an exponential was fit to the Morse potential at 4 bohr (2.117×10^{-10} m) and the orthogonalized valence-bond potential (table I) at 2.5 bohr (1.323×10^{-10} m) (see fig. 5).

The dipole moment integrals were integrated on a digital computer between $R = 0$ and 25 bohr (0 and 13.23×10^{-10} m) and are given in table II.

Integrated Absorption Coefficients

Equations (35) to (42) were used to calculate the integrated absorption coefficients S of transitions with a net change in vibrational quanta of +1. Vibration-rotation term values were obtained by adding rotational term values of Patch (ref. 33) to vibrational term values of Spindler (ref. 34). Only states with energies below the dissociation energy were included. Vibrating-rotator vibrational overlap integrals and matrix elements were calculated on a digital computer using Spindler's potential energy to which $\frac{h^2 J(J+1)}{8\pi^2 m_r r^2}$ was added. Typical vibrational matrix elements are shown in figures 6 and 7 and are compared with harmonic-oscillator rigid-rotator vibrational matrix elements used by all previous investigators. For large values of J the two models give very different values. Some vibrational overlap integrals are shown in figures 8 and 9 and are compared with harmonic-oscillator rigid-rotator overlap integrals used by all previous investigators. Again there are some large differences. The vibrating-rotator matrix elements and overlap integrals agree well with James (ref. 35). It would be reasonable to expect that the large differences between the results from the two models would have large effects on S .

Preliminary integrated absorption coefficients S for 298 and 5200 K obtained by evaluating equations (35) to (42) on a digital computer showed that certain transitions could be neglected. Double vibrational transitions where one molecule had a change of +2 vibrational quanta and the other had a change of -1 vibrational quanta had negligible S values. Because of this and because all double vibrational transitions are forbidden for the harmonic-oscillator rigid-rotator model, all double vibrational transitions were henceforth neglected, and only single vibrational transitions where one molecule had a change of +1 vibrational quanta were included. In the latter, double rotational transitions had negligible S values and were therefore excluded in the final program. However, the final program did include double transitions in which there was a vibrational transition in one molecule and a rotational transition in the other molecule.

Final integrated absorption coefficients summed over all values of v_1 , v_2 , J_1 , and J_2 are given in figure 10. At all temperatures most of the contribution to the total integrated absorption coefficient is due to Q branches.

A comparison of values of S for single vibrational transitions with a change in v of +1 for three models is given in figure 11. The vibrating-rotator model gave S as much as 30 percent higher than the simpler harmonic-oscillator rigid-rotator model. A hybrid model with vibrating-rotator term values and partition functions and with harmonic-oscillator rigid-rotator vibrational overlap integrals and matrix elements is also included.

Spectral Absorption Coefficients

The spectral absorption coefficient with wave number removed was calculated from S by equations (48) to (57) and is given in figure 12 for the vibrating-rotator model for single vibrational transitions with a change in v of +1. The major peaks are due to Q branches. The small bump in the 600 K curve at about 4700 reciprocal centimeters is due to S branches. The small bump in the 7000 K curve at about 500 reciprocal centimeters is due to O branches. The major peak shifts to smaller wave numbers as temperature is increased because of the smaller wave numbers of Q-lines with excited initial states, the increased importance of O-branches at high temperature, and the decreased importance of S branches at high temperature.

Once the absorption coefficient has been calculated accurately for a number of temperatures and wave numbers, it can be calculated much more rapidly for any temperature or wave number in the same range by using an approximate fit to the accurate results. The absorption coefficient $\tilde{A}_{\tilde{\nu}}$ can be approximated by a modified Q-line shape.

$$\tilde{A}_{\tilde{\nu}} \approx \frac{\gamma w_1^2 \exp\left[j(\tilde{\nu} - \tilde{\nu}_c)\right]}{(\tilde{\nu} - \tilde{\nu}_c)^2 + w_1^2} \quad (\tilde{\nu} < \tilde{\nu}_c) \quad (58)$$

$$\tilde{A}_{\tilde{\nu}} \approx \frac{\gamma w_2^2}{(\tilde{\nu} - \tilde{\nu}_c)^2 + w_2^2} \quad \left(\tilde{\nu}_c \leq \tilde{\nu} \leq \tilde{\nu}_c + \frac{3}{2}w_2\right) \quad (59)$$

$$\tilde{A}_{\tilde{\nu}} \approx b \exp\left[\frac{-(\tilde{\nu} - \tilde{\nu}_c)}{g}\right] \quad \left(\tilde{\nu}_c + \frac{3}{2}w_2 \leq \tilde{\nu}\right) \quad (60)$$

where the wave number $\tilde{\nu}_c$ of the line center is given by

$$\log_{10}(4172 - \tilde{\nu}_c) = -5.1972 + 2.1 \log_{10} T \quad (61)$$

and

$$\gamma = 6.0273 \times 10^{-10} + 2.2905 \times 10^{-13} T + 4.0848 \times 10^{-17} T^2 \quad (62)$$

$$w_1 = 363.96 + 1.3530 T - 3.5807 \times 10^{-4} T^2 + 3.3618 \times 10^{-8} T^3 \quad (63)$$

$$\log_{10} j = 161.45 T^{-1} - 2.6996 - 1.9537 \times 10^{-4} T \quad (64)$$

$$w_2 = -108626 T^{-1} + 697.59 + 0.14353 T \quad (65)$$

$$\log_{10} b = 28.765 T^{-1} - 9.0461 + 1.1552 \times 10^{-4} T \quad (66)$$

$$\log_{10} g = 1.4860 + 0.44462 \log_{10} T \quad (67)$$

The constants in equations (61) to (67) were determined by fitting the absorption coefficients in figure 12 and similar data for wave numbers from 8000 to 40 000 reciprocal centimeters and are valid for temperatures between 600 and 7000 K and wave numbers between 100 and 40 000 reciprocal centimeters. In equations (58) to (67) temperature is in degrees Kelvin, and wave number is in reciprocal centimeters. On a high-speed digital computer the use of equations (58) to (67) instead of equations (33) to (40), (42), and (48) to (57) results in two orders of magnitude less running time, one-fifth the storage locations, and accuracy at any wave number within ± 10 percent of the maximum value $\tilde{A}_{\tilde{\nu}}$ for the given temperature.

From equations (46) and (47) the attenuation of a monochromatic light beam by a path length l in H_2 gas in terms of $\tilde{A}_{\tilde{\nu}}$ is

$$\frac{I}{I_0} = \exp \left[-\tilde{A}_{\tilde{\nu}} \tilde{\nu} \left(1 - e^{-hc\tilde{\nu}/kT} \right) \rho^2 l \right] \quad (68)$$

where $\tilde{A}_{\tilde{\nu}}$ and ρ are dimensionless.

For quick reference $A_{\tilde{\nu}}$ is more convenient than $\tilde{A}_{\tilde{\nu}}$ and was obtained from $\tilde{A}_{\tilde{\nu}}$ by equation (46). The results for the vibrating-rotator model are shown in figure 13.

The calculation of $\tilde{A}_{\tilde{\nu}}$ and $A_{\tilde{\nu}}$ is greatly complicated by using the vibrating-rotator model rather than the harmonic-oscillator rigid-rotator model, so it is interesting to see how this affects the answer. This is shown in figure 14 for 4000 K. A hybrid model is also included in figure 14. The principal effect of using the vibrating-rotator model rather than the harmonic-oscillator rigid-rotator model is to shift the absorption to smaller wave numbers.

Comparison with Other Investigators

Hare and Welsh (ref. 10) measured the binary and ternary integrated absorption coefficients for the H_2 fundamental at 298 K. After allowing for their different definition of the integrated absorption coefficient, we find the vibrating-rotator model gives 87 per cent of their value for the binary integrated absorption coefficient. The discrepancy is principally due to the neglect of x and y components of the dipole moment derivative in the vibrating-rotator model.

Linsky (ref. 7) calculated $A_{\tilde{\nu}}$ by extrapolating Van Kranendonk's (ref. 6) theory. The vibrating-rotator model is compared with Linsky's model in figure 15 for 3000 K. The vibrating-rotator model (labelled "This report") has an integrated absorption coefficient 2.1 times Linsky's value. However, this is not so much due to the vibrating-rotator model itself as to the intermolecular potential used with it (see fig. 5). Linsky followed Van Kranendonk (ref. 6) in using the unrealistic Lennard-Jones 6-12 potential also shown in figure 5.

Linsky's pressure-induced translational, rotational, and vibrational absorption coefficients together with absorption coefficients for 12 other processes were used by Patch (ref. 36) to calculate the Planck and Rosseland mean opacities of hydrogen. The results are shown in figures 16 and 17. The discontinuities in the curves at 3000 K are because Linsky gave no vibrational absorption coefficients above this temperature. Patch's calculation (ref. 36) was repeated using equations (58) to (67) for pressure-induced vibrational absorption instead of Linsky's. The resulting opacities for pressures of 100 and 1000 atmospheres (1.013×10^7 and 1.013×10^8 N/m²) are labelled "This report" in figures 16 and 17. Below 3000 K equations (58) to (67) resulted in Planck and Rosseland mean opacities as much as factors of 1.9 and 303 higher, respectively, than in reference 36. Above 3000 K equations (58) to (67) resulted in Planck and Rosseland mean opacities as much as factors of 18.9 and 6.5 higher, respectively, than in reference 36.

Effect on Gaseous-Core Nuclear Rockets

The opacity of hydrogen (figs. 16 and 17) is still not enough below 6000 K to obtain

adequate heat transfer to hydrogen and to protect the walls of gaseous-core nuclear rockets. Some opaque additive to the hydrogen would be necessary.

CONCLUSIONS

The coefficient for pressure-induced vibrational absorption in $H_2 - H_2$ collisions was calculated for temperatures between 298 and 7000 K and wave numbers from 100 to 40 000 reciprocal centimeters with many refinements. The conclusions were

1. The integrated absorption coefficient at 298 K was 87 percent of the experimental value.

2. At 3000 K the integrated absorption coefficient was 2.1 times a previous theoretical estimate, principally due to use of a more realistic intermolecular potential in this report.

3. Although the vibrating-rotator model gave quite different vibrational matrix elements and overlap integrals compared to the usual harmonic-oscillator rigid-rotator model, it did not cause more than a 30-percent change in the integrated absorption coefficient.

4. The vibrating-rotator model shifted the absorption to smaller wave numbers than for the harmonic-oscillator rigid-rotator model.

5. Below 3000 K, where a previous estimate of vibrational absorption was available, absorption coefficients from this report resulted in Planck and Rosseland mean opacities as much as factors of 1.9 and 303, higher, respectively, than the best previous estimates for pressures from 100 to 1000 atmospheres (1.013×10^7 to 1.013×10^8 N/m²).

6. Above 3000 K, where no previous estimate of vibrational absorption was available, absorption coefficients from this report resulted in Planck and Rosseland mean opacities as much as factors of 18.9 and 6.5, higher, respectively, than the best previous estimates for pressures from 100 to 1000 atmospheres (1.013×10^7 to 1.013×10^8 N/m²).

7. The opacity of hydrogen below 6000 K is still not enough to obtain adequate heat transfer to hydrogen and to protect the walls of gaseous-core nuclear rockets. Some opaque additive to the hydrogen would be necessary.

Lewis Research Center,

National Aeronautics and Space Administration,

Cleveland, Ohio, October 20, 1970,

122-28.

APPENDIX - SYMBOLS

$A_{\tilde{\nu}}$	spectral absorption coefficient including wave number and stimulated emission
$\tilde{A}_{\tilde{\nu}}$	spectral absorption coefficient with wave number removed and excluding stimulated emission
$A_{ij}(k)$	function of molecule k involving integral of normalized associated Legendre functions
$a_{\tilde{\nu}}$	linear absorption coefficient for wave number $\tilde{\nu}$ excluding stimulated emission
B	integrated Einstein coefficient of absorption
$B_{\tilde{\nu}}$	spectral Einstein coefficient of absorption
b	function of temperature in modified Q-line shape
$C_{l_1 \xi_1 l_2 \xi_2}$	expansion coefficient for μ_z^0
c	speed of light
$c_i (i=1, 2, 3, 4)$	constants for faired curve
$D_{l_1 \xi_1 l_2 \xi_2}$	expansion coefficient for μ_1
$E_i (i=1, 9)$	product of two expansion coefficients
e	charge of electron
F	constant in Q-branch line shape
$f_{\tilde{\nu}}$	line shape function
G	constant in O- and S-branch line shape
$G_i (i=1, 2, 3, 45)$	functions of Q , Δ , and I
g	function of temperature in modified Q-line shape
H	constant in O- and S-branch line shape
h	Planck constant
$I_i (i=1, 2, \dots, 9)$	dipole moment integral
I	transmitted light intensity
I_0	incident light intensity
i	$\sqrt{-1}$

$J_i(i=1, 2)$	total angular momentum quantum number for initial state of molecule i
$J'_i(i=1, 2)$	total angular momentum quantum number for final state of molecule i
j	function of temperature in modified Q-line shape
k	Boltzmann constant
$L_i(i=0, 2)$	functions of J' and J
l	path length
M	constant in O- and S-branch line shape
$M_i(i=1, 2, \dots, 5)$	functions of Q , Δ , C , and D
$m_i(i=1, 2)$	quantum number for component of total angular momentum along z axis for initial state of molecule i
$m'_i(i=1, 2)$	quantum number for component of total angular momentum along z axis for final state of molecule i
m_r	reduced mass of oscillator
N	number of H_2 molecules
n	number density of H_2 molecules
n_0	Loschmidt number
$P(v_i, J_i, m_i) \Big\{ (i=1, 2) \Big\}$	probability of molecule i being in state with quantum numbers having values v_i, J_i, m_i
p	number of pairs of molecules
$Q_k(k=1, 2)$	vibrational overlap integral for molecule k
R	intermolecular distance
$r_k(k=1, 2)$	internuclear distance of molecule k
S	integrated absorption coefficient with wave number and density removed
s	integrated absorption coefficient with wave number removed
T	temperature
t	time
U	constant in Q-branch line shape
V	volume

$v_i(i=1, 2)$	vibrational quantum number for initial state of molecule i
$v_i'(i=1, 2)$	vibrational quantum number for final state of molecule i
W	transition-dependent factor in s
w_Q, w_S, w_1, w_2	line widths
x, y, z	Cartesian coordinates fixed in space (fig. 1)
X_i	position coordinates of electrons
Y_{Jm}	spherical harmonic
Z_j	number of elemental charges on the j^{th} nucleus
z_i	z coordinate of i^{th} electron
z_j	z coordinate of j^{th} nucleus
γ	function of temperature in modified Q-line shape
$\Delta_k(k=1, 2)$	vibrational matrix element for molecule k
$\delta(J', J)$	Kronecker delta function
ϵ_0	electric permittivity of free space
Θ_{Jm}	normalized associated Legendre function
$\theta_i(i=1, 2)$	polar angle of molecule i
μ_x, μ_y, μ_z	components of electric dipole moment
$\mu_i'(i=1, 2)$	$\partial\mu_z/\partial r_i$ evaluated at $r_1 = r_1^0$ and $r_2 = r_2^0$
$\mu_z, 4$	μ_z for configuration 4
$\left. \begin{array}{l} (\mu_x)_{\rho'\rho} \\ (\mu_y)_{\rho'\rho} \\ (\mu_z)_{\rho'\rho} \end{array} \right\}$	components of electric dipole moment matrix elements
$\tilde{\nu}$	photon wave number
$\tilde{\nu}_0, \tilde{\nu}_c$	wave number of line center
ρ	dimensionless H_2 density (see eq. (43))
$\rho\tilde{\nu}$	radiation energy density per unit wave number
$d\tau$	element of volume in configuration space
Φ	intermolecular potential averaged over orientations

φ_i (i=1, 2) azimuthal angle of molecule i
 ψ wave function
 $\psi_{v_k J_k}$ (k=1, 2) vibrational wave function of molecule k

Subscripts:

e electronic
 n nuclear
 ζ v_1, v_2, J_1, J_2 collectively
 ζ' v'_1, v'_2, J'_1, J'_2 collectively
 ρ $v_1, v_2, J_1, J_2, m_1, m_2$ collectively
 ρ' $v'_1, v'_2, J'_1, J'_2, m'_1, m'_2$ collectively

Superscripts:

o equilibrium internuclear distance of diatomic molecule
 * complex conjugate

REFERENCES

1. Anon.: Proceedings of the NASA-University Conference on the Science and Technology of Space Exploration. NASA SP-11, Vol. 2, 1962, pp. 61-122.
2. Kascak, Albert F.; and Easley, Annie J.: Effect of Turbulent Mixing on Average Fuel Temperatures in a Gas-Core Nuclear Rocket Engine. NASA TN D-4882, 1968.
3. Van Kranendonk, J.; and Bird, R. Byron: Pressure-Induced Absorption. I. The Calculation of Pressure-Induced Absorption in Pure Hydrogen and Deuterium. *Physica*, vol. 17, nos. 11-12, Nov.-Dec. 1951, pp. 953-967.
4. Britton, F. R.; and Crawford, M. F.: The Theory of Collision-Induced Absorption in Hydrogen and Deuterium. *Can. J. Phys.*, vol. 36, no. 6, June 1958, pp. 761-783.
5. Van Kranendonk, J.: Theory of Induced Infra-Red Absorption. *Physica*, vol. 23, no. 10, Oct. 1957, pp. 825-837.
6. Van Kranendonk, J.: Induced Infra-Red Absorption in Gases. Calculation of the Binary Absorption Coefficients of Symmetrical Diatomic Molecules. *Physica*, vol. 24, no. 3, Mar. 1958, pp. 347-362.
7. Linsky, Jeffrey L.: On the Pressure-Induced Opacity of Molecular Hydrogen in Late-Type Stars. *Astrophys. J.*, vol. 156, no. 3, June 1969, pp. 989-1005.
8. Hirschfelder, Joseph O.; Curtiss, Charles F.; and Bird, R. Byron: *Molecular Theory of Gases and Liquids*. John Wiley & Sons, Inc., 1954, pp. 1110-1113.
9. Gush, H. P.; Nanassy, A.; and Welsh, H. L.: Structure of the Fundamental Infra-red Band of Hydrogen in Pressure Induced Absorption. *Can. J. Phys.*, vol. 35, no. 6, June 1957, pp. 712-719.
10. Hare, W. F. J.; and Welsh, H. L.: Pressure-Induced Infrared Absorption of Hydrogen and Hydrogen-Foreign Gas Mixtures in the Range 1500-5000 Atmospheres. *Can. J. Phys.*, vol. 36, no. 1, Jan 1958, pp. 88-103.
11. Hunt, J. L.; and Welsh, H. L.: Analysis of the Profile of the Fundamental Infrared Band of Hydrogen in Pressure-Induced Absorption. *Can. J. Phys.*, vol. 42, no. 5, May 1964, pp. 873-885.
12. Patch, R. W.: Calculated Interaction Energy and Dipole Moment in Collisions of Two Hydrogen Molecules. NASA TN D-5486, 1969.
13. Patch, R. W.: Semiempirical Electric Dipole Moment and its Derivative in $H_2 - H_2$ and $H_2 - H$ Collisions. NASA TN D-5994, 1970.

14. Chandrasekhar, S.: An Introduction to the Study of Stellar Structure. Dover Publ., Inc., 1957, p. 191.
15. Davidson, Norman R.: Statistical Mechanics. McGraw-Hill Book Co., Inc., 1962, pp. 471-475.
16. Wilson, E. Bright, Jr.; Decius, J. C.; and Cross, Paul C.: Molecular Vibrations; The Theory of Infrared and Raman Vibrational Spectra. McGraw-Hill Book Co., Inc., 1955, p. 38.
17. Slater, John C.: Quantum Theory of Molecules and Solids. Vol. 1. Electronic Structure of Molecules. McGraw-Hill Book Co., Inc., 1963, pp. 9-253.
18. Patch, R. W.; and McBride, Bonnie J.: Partition Functions and Thermodynamic Properties to High Temperatures for H_3^+ and H_2^+ . NASA TN D-4523, 1968.
19. Pauling, Linus; and Wilson, E. Bright: Introduction to Quantum Mechanics with Applications to Chemistry. McGraw-Hill Book Co., Inc., 1935, pp. 134-135.
20. Bethe, Hans A.; and Salpeter, Edwin E.: Quantum Mechanics of One- and Two-Electron Atoms. Academic Press, 1957, pp. 344-347.
21. Poll, Jacobus D.: Theory of Translational Effects in Induced Infrared Spectra. Ph.D. Thesis, Univ. Toronto, 1960.
22. Watanabe, A.; and Welsh, H. L.: Pressure-Induced Infrared Absorption of Gaseous Hydrogen and Deuterium at Low Temperatures. II. Analysis of the Band Profiles for Hydrogen. Can. J. Phys., vol. 45, no. 9, Sept. 1967, pp. 2859-2871.
23. MacTaggart, John W.; and Hunt, James L.: An Analysis of the Profile of the Pressure-Induced Pure Rotational Spectrum of Hydrogen Gas. Can. J. Phys., vol. 47, no. 1, Jan 1969, pp. 65-70.
24. Fisher, B. B.: Calculations of the Thermal Properties of Hydrogen. Rep. LA-3364, Los Alamos Scientific Lab., Apr. 20, 1966.
25. Geuvara, F. A.; and Wageman, W. E.: Measurement of Helium and Hydrogen Viscosities to 2340 K. Rep. LA-3319, Los Alamos Scientific Lab., Sept. 2, 1965.
26. Johnston, Herrick L.; and McCloskey, Kenneth E.: Viscosities of Several Common Gases Between 90 K and Room Temperature. J. Phys. Chem., vol. 44, no. 9, Dec. 1940, pp. 1038-1058.
27. Trautz, Max; and Baumann, P. B.: Die Reibung, Wärmeleitung und Diffusion in Gasmischungen. II. Die Reibung von H_2 - N_2 - und H_2 - CO - Gemischen. Ann. Physik, vol. 2, no. 6, Aug. 26, 1929, pp. 733-736.

28. Trautz, Max; and Heberling, Robert: Die Reibung, Wärmeleitung und Diffusion in Gasmischungen. XXV. Die innere Reibung von Xenon und seinen Gemischen mit Wasserstoff und Helium. Ann. Physik, vol. 20, no. 2, June 6, 1934, pp. 118-120.
29. Trautz, Max; and Husseini, Ishaq: Die Reibung, Wärmeleitung und Diffusion in Gasmischungen. XXVI. Die innere Reibung von Propylen und β - Butylen und von ihren Mischungen mit He oder H₂. Ann. Physik, vol. 20, no. 2, June 6, 1934, pp. 121-126.
30. Trautz, Max; and Binkele, H. E.: Die Reibung, Wärmeleitung und Diffusion in Gasmischungen. VIII. Die Reibung des H₂, He, Ne, Ar und ihrer binären Gemische. Ann. Physik, vol. 5, no. 5, June 28, 1930, pp. 561-580.
31. Wobser, R.; and Müller, Fr.: Die innere Reibung von Gasen und Dämpfen und ihre Messung im Höppler-Viskosimeter. Kolloid-Beih., vol. 52, no. 6-7, Feb. 4, 1941, pp. 165-276.
32. Woolley, Harold W.; Scott, Russell, B.; and Brickwedde, F. G.: Compilation of Thermal Properties of Hydrogen in its Various Isotopic and Ortho-Para Modifications. J. Res. Nat. Bur. Std., vol. 41, no. 5, Nov. 1948, pp. 379-475.
33. Patch, R. W.: Components of a Hydrogen Plasma Including Minor Species. NASA TN D-4993, 1969.
34. Spindler, R. J., Jr.: Franck-Condon Factors for Band Systems of Molecular Hydrogen. I. The

$$\left(B \ 1_{\Sigma_u^+} - X \ 1_{\Sigma_g^+} \right), \left(I \ 1_{\pi_g} - B \ 1_{\Sigma_u^+} \right) \text{ and } \left(d \ 3_{\pi_u} - a \ 3_{\Sigma_g^+} \right)$$

Systems. J. Quant. Spectrosc. Radiat. Transfer, vol. 9, no. 5, May 1969, pp. 597-626.

35. James, Thomas C.: Exact Vibrational Matrix Elements for Molecular Hydrogen and the Intensity of the Quadrupole Rotation - Vibration Spectrum. Astrophys. J., vol. 146, no. 2, Nov. 1966, pp. 572-580.
36. Patch, R. W.: Interim Absorption Coefficients and Opacities for Hydrogen Plasma at High Pressure. NASA TM X-1902, 1969.

TABLE I. - DIPOLE MOMENT EXPANSION COEFFICIENTS AND INTERMOLECULAR POTENTIAL FROM ORTHOGONALIZED VALENCE-BOND CALCULATIONS

Inter-molecular distance, R, m	Expansion coefficient						Inter-molecular potential, Φ , J
	C_{2000}' , C m	D_{0000}' , C	D_{2000}' , C	D_{0020}' , C	D_{2020}' , C	D_{2-222}' , C	
1.323×10^{-10}	1.758×10^{-30}	9.806×10^{-20}	6.351×10^{-20}	-0.169×10^{-20}	-0.121×10^{-20}	0.077×10^{-20}	6.210×10^{-19}
1.588	9.510×10^{-31}	5.609	3.709	-.169	.009	.045	2.645
1.852	4.947	2.986	1.996	-.172	.004	.027	1.127
2.117	2.498	1.516	1.024	-.130	-.006	.016	4.732×10^{-20}

TABLE II. - DIPOLE MOMENT INTEGRALS

Temperature, T, K	Dipole moment integral								
	I_1' , $C^2 m^3$	I_2' , $C^2 m^3$	I_3' , $C^2 m^3$	I_4' , $C^2 m^3$	I_5' , $C^2 m^3$	I_6' , $C^2 m^5$	I_7' , $C^2 m^4$	I_8' , $C^2 m^4$	I_9' , $C^2 m^3$
600	9.980×10^{-70}	4.845×10^{-70}	4.781×10^{-71}	2.339×10^{-73}	5.534×10^{-74}	4.368×10^{-91}	1.415×10^{-80}	-4.418×10^{-81}	-1.349×10^{-70}
1000	1.543×10^{-69}	7.325	5.363	2.550	1.085×10^{-73}	5.780	2.007	-5.313	-1.727
2000	2.991	1.389×10^{-69}	6.519	2.889	2.498	9.653	3.603	-7.370	-2.580
3000	4.515	2.076	7.397	3.123	3.891	1.380×10^{-90}	5.291	-9.186	-3.323
4000	6.074	2.774	8.090	3.316	5.230	1.809	7.022	-1.080×10^{-80}	-3.978
5000	7.648	3.475	8.656	3.494	6.511	2.247	8.773	-1.225	-4.564
6000	9.227	4.176	9.136	3.674	7.747	2.688	1.053×10^{-79}	-1.357	-5.096
7000	1.079×10^{-68}	4.868	9.542	3.876	8.938	3.131	1.228	-1.478	-5.583

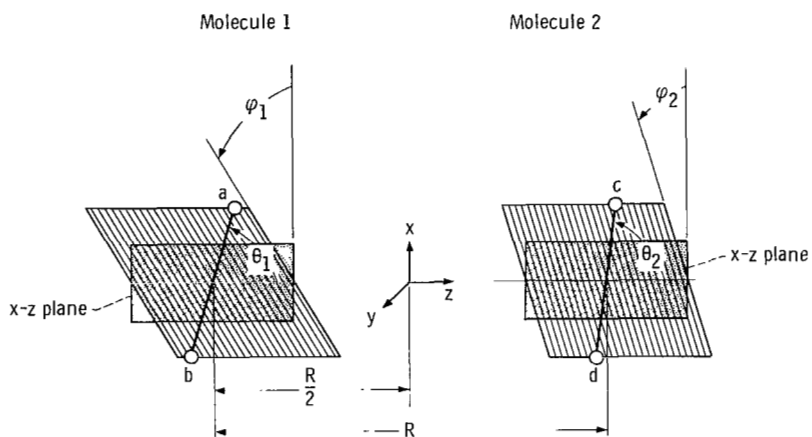


Figure 1. - Cartesian and polar coordinates for collisions of two H_2 molecules. Protons are located at a, b, c, and d. The z axis passes through the midpoints of the molecules. The angles θ_1 and θ_2 are polar angles. The angles ϕ_1 and ϕ_2 are azimuthal angles measured in the x-y plane.

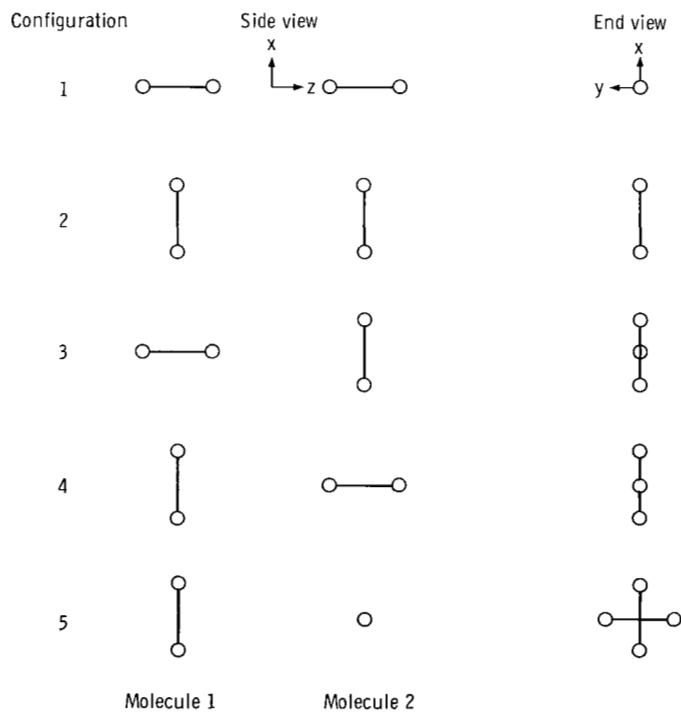


Figure 2. - Configurations of two H_2 molecules for which $\mu_2^0(R)$ and $\mu_1(R)$ are required by the theory in this report.

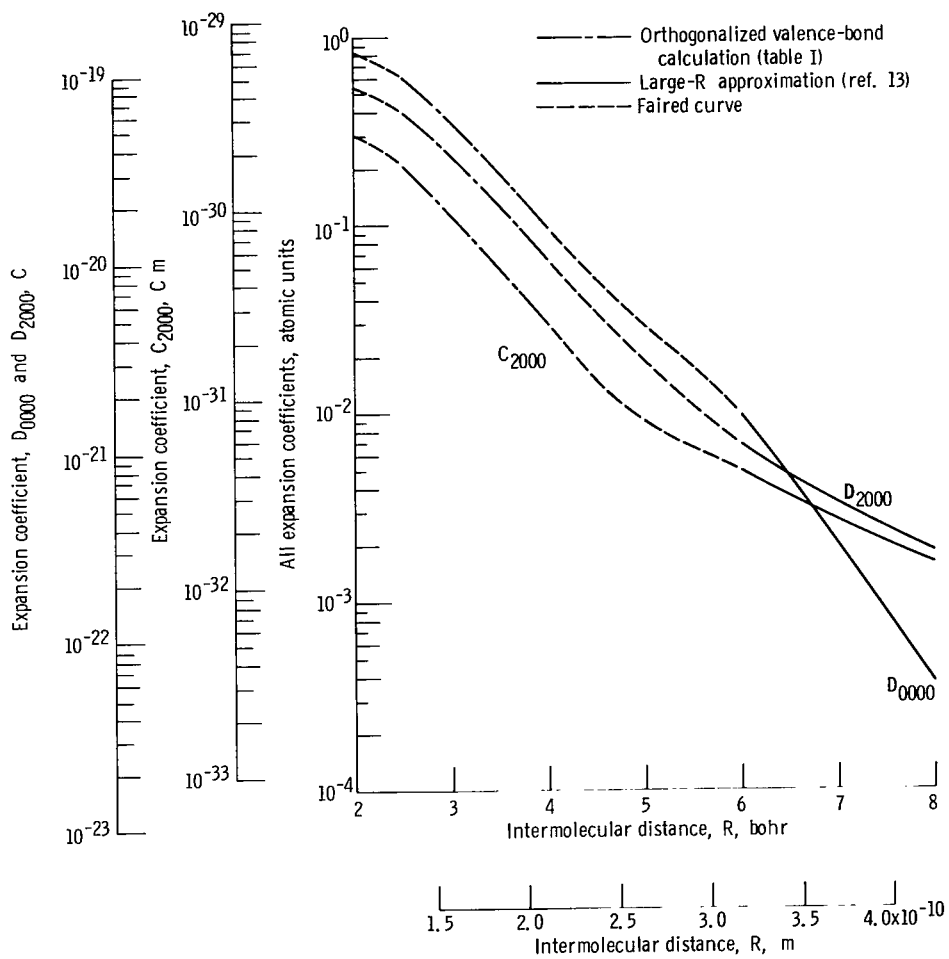


Figure 3. - The three largest expansion coefficients of the dipole moment and its derivative.

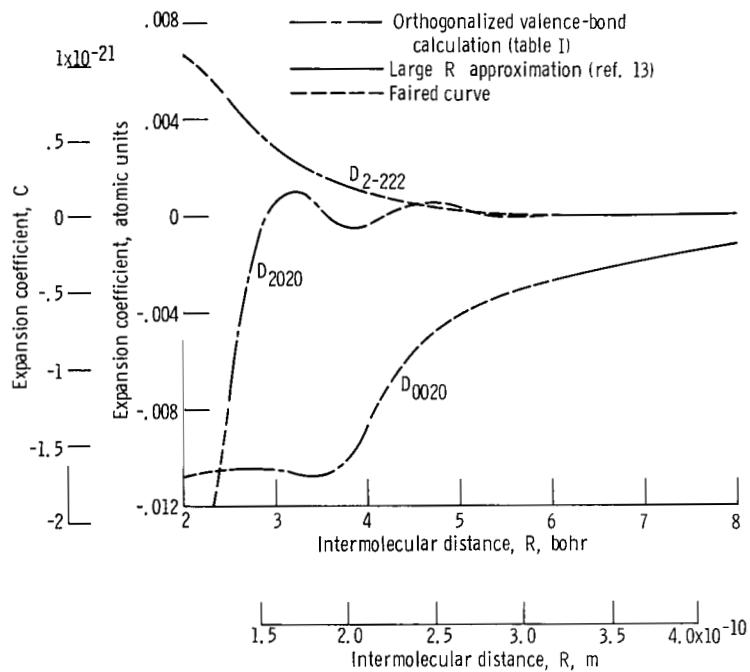


Figure 4. - The three smallest and least important expansion coefficients of the derivative of the dipole moment. The oscillation of D_{2020} results partly from the interpolation formula used between the four points from orthogonalized valence-bond calculations and may not be entirely valid. However, D_{2020} makes a negligible contribution to the pressure-induced vibrational absorption coefficient.

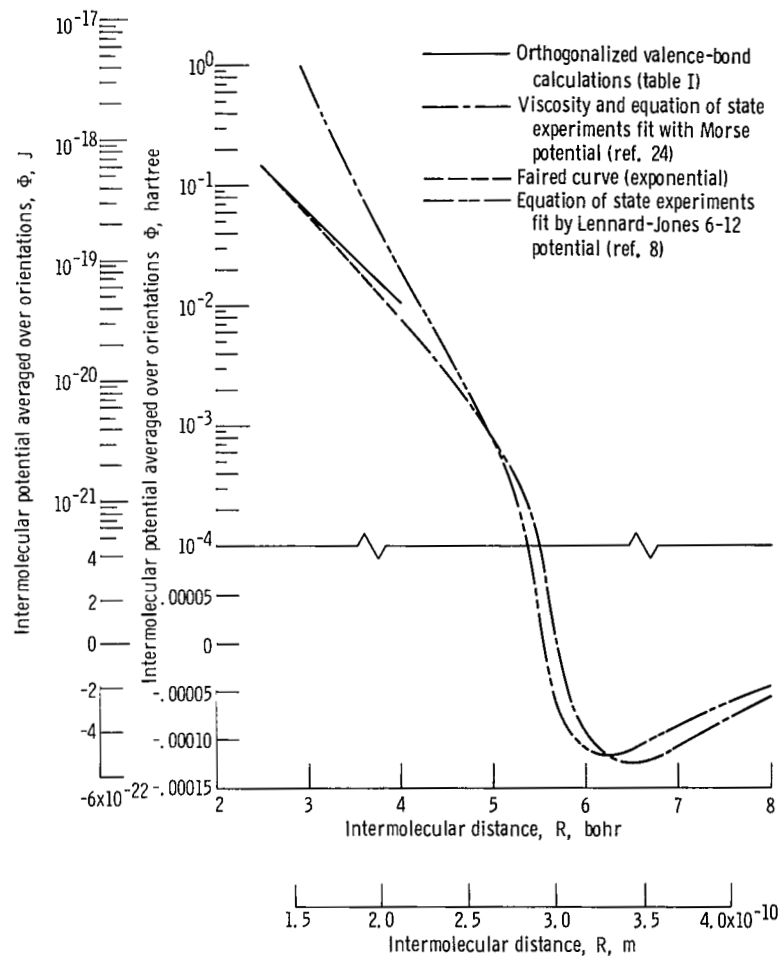


Figure 5. - H_2-H_2 intermolecular potential from several sources.

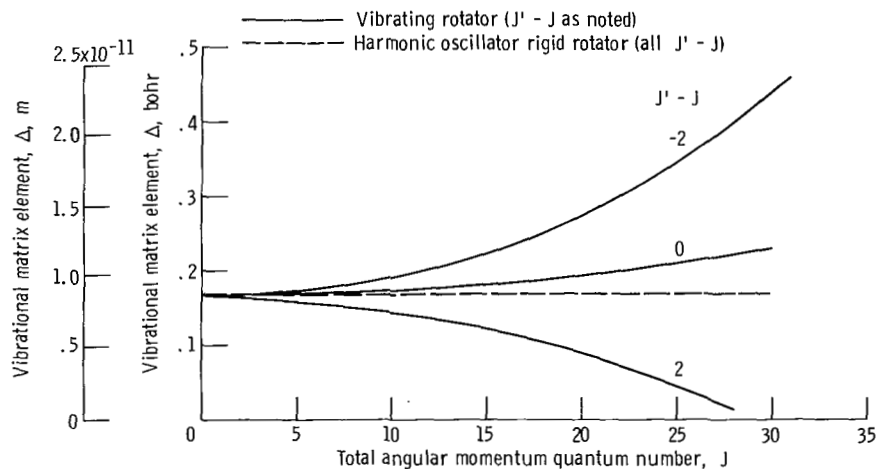


Figure 6. - Vibrational matrix elements for H_2 for $v = 0$ and $v' = 1$ for two models show the effect of vibration-rotation interaction.

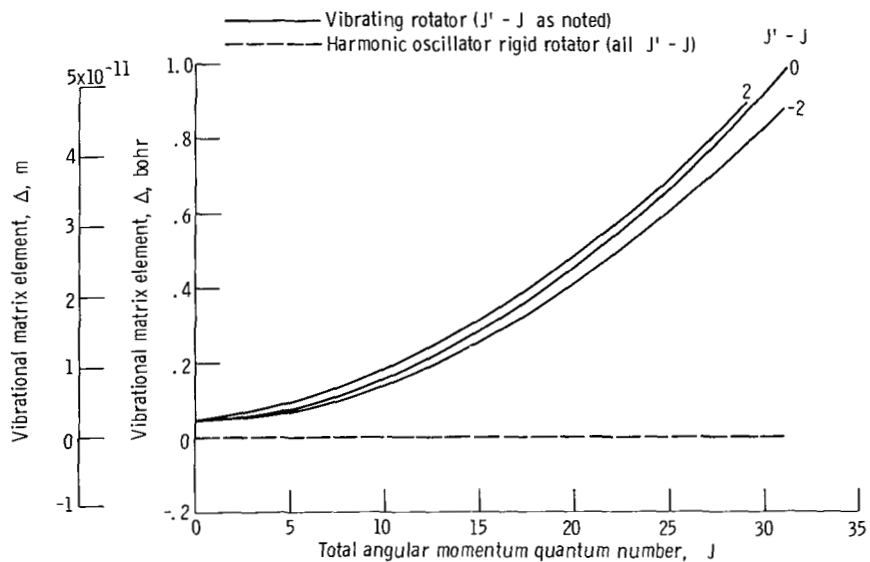


Figure 7. - Vibrational matrix elements for H_2 for $v = 0$ and $v' = 0$ for two models show the effect of mechanical anharmonicity and vibration rotation interaction.

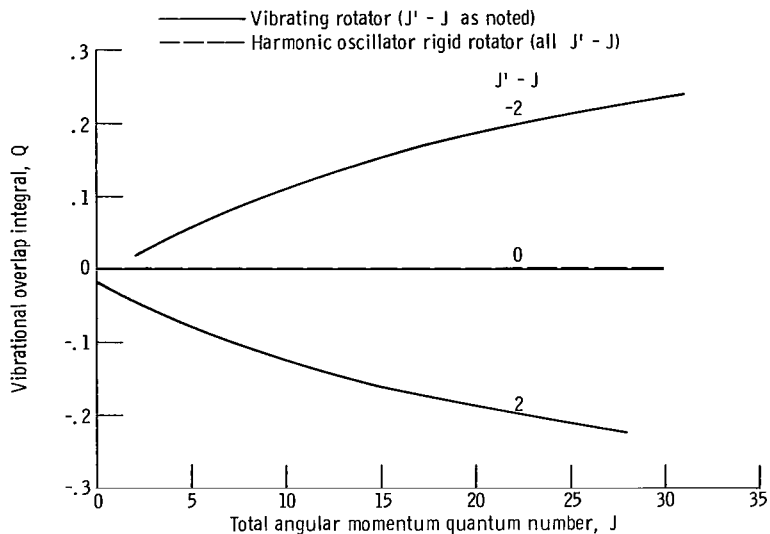


Figure 8. - Vibrational overlap integrals for H_2 for $v = 0$ and $v' = 1$ for two models show the effect of vibration-rotation interaction. The harmonic-oscillator rigid-rotator line coincides with the vibrating-rotator line for $J' - J = 0$.

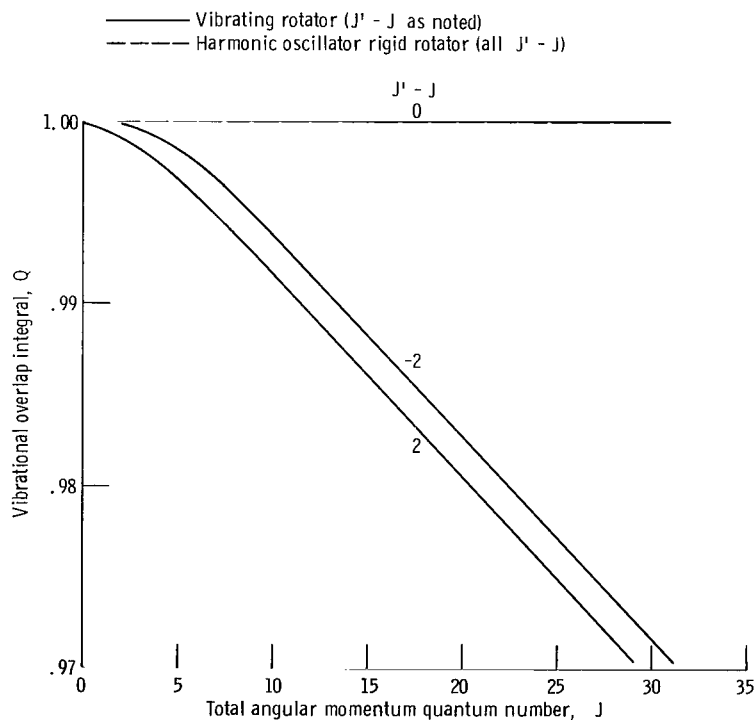


Figure 9. - Vibrational overlap integrals for H_2 for $v = 0$, $v' = 0$ for two models show the effect of vibration-rotation interaction. The harmonic-oscillator rigid-rotator line coincides with the vibrating-rotator line for $J' - J = 0$.

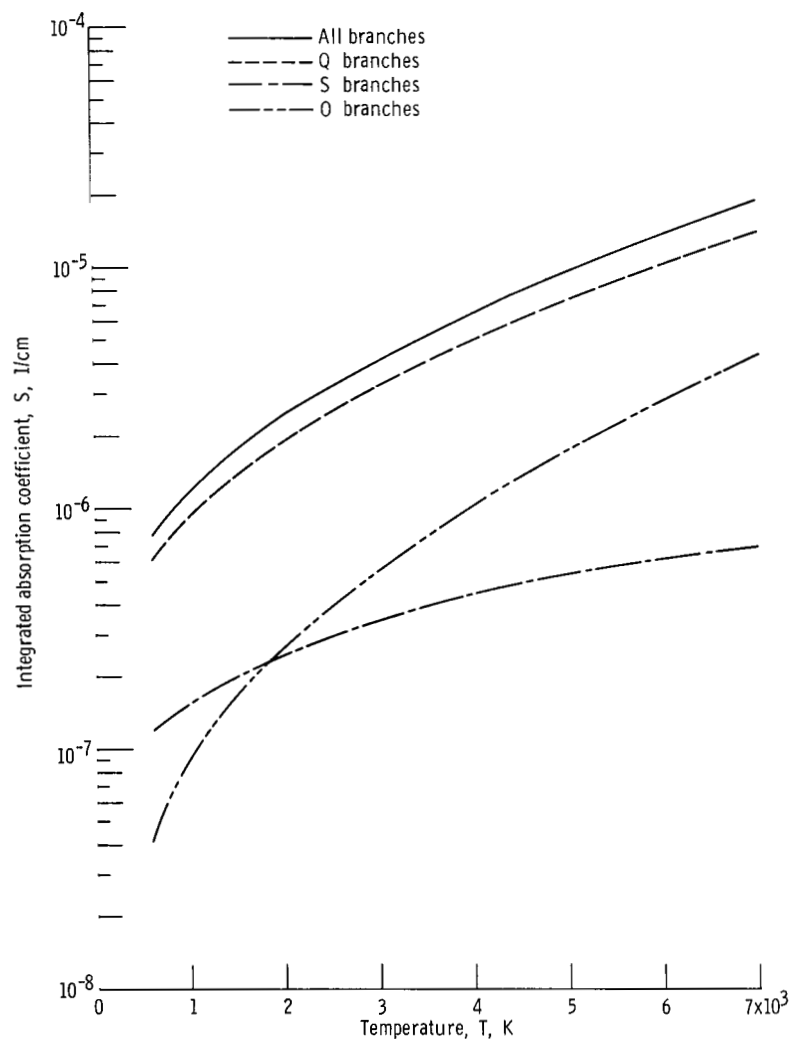


Figure 10. - Integrated absorption coefficient for various branches of all single vibrational transitions with a change in v of +1. The total for all branches is also given. The vibrating-rotator model was used.

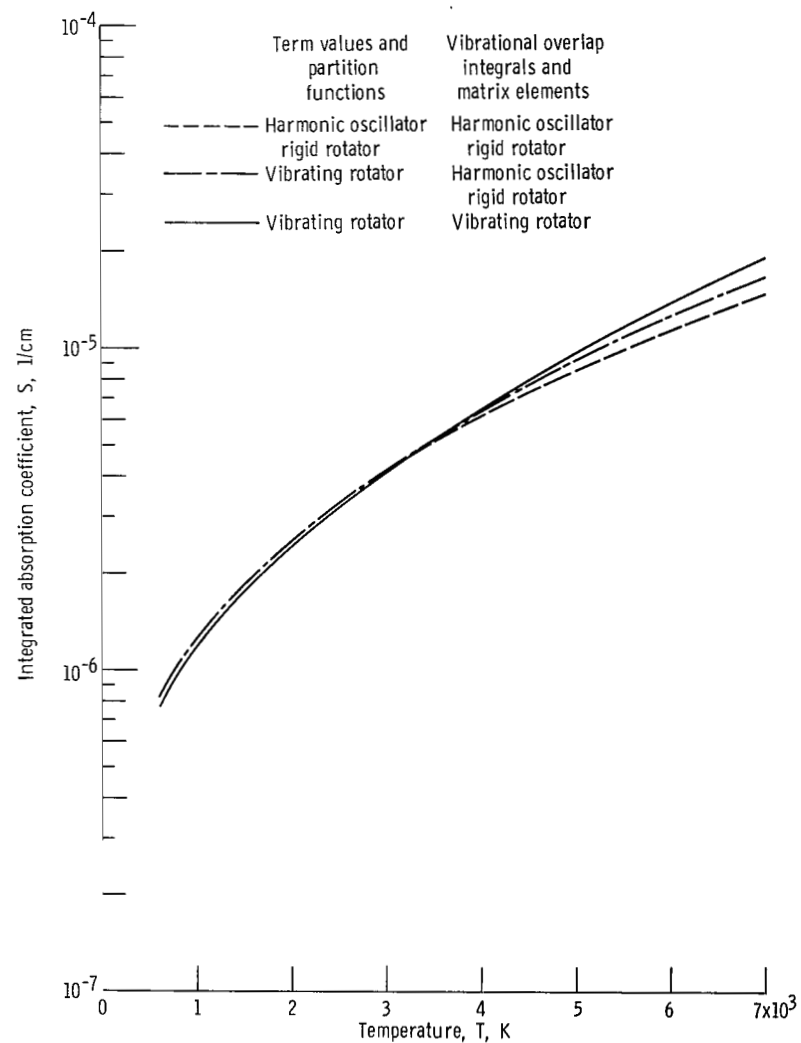


Figure 11. - Integrated absorption coefficient for all single vibrational transitions with a change in v of +1, using three models. The --- and -.- curves coincide for temperatures below 3000 K.

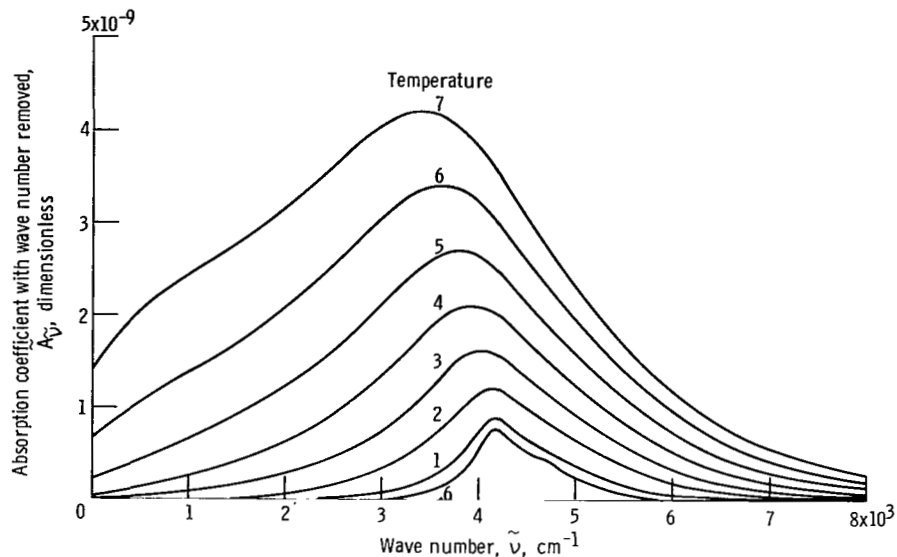


Figure 12. - Calculated pressure-induced vibrational absorption coefficient for all single vibrational transitions with a change in v of $+1$. The wave number has been removed from the absorption coefficient in the manner customary for pressure-induced processes. The effect of stimulated emission is not included. Temperature is given in thousands of degrees Kelvin.

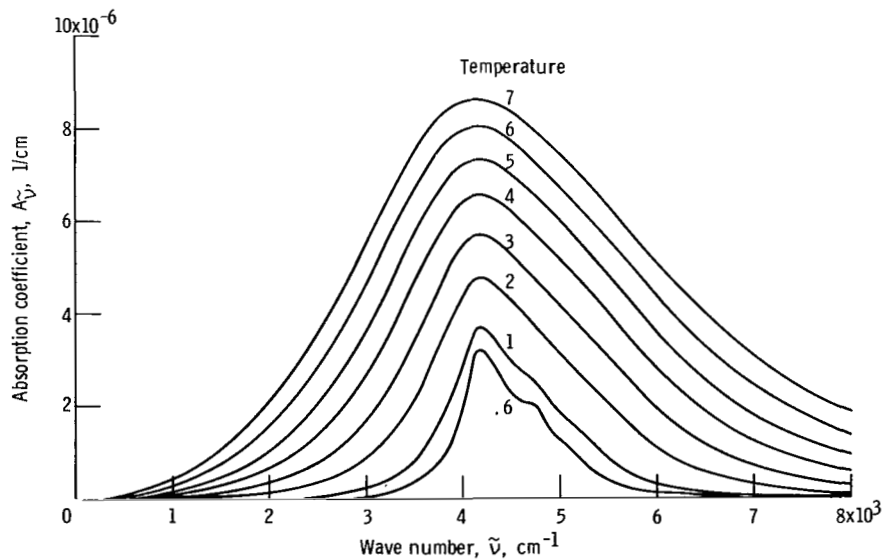


Figure 13. - Calculated pressure-induced vibrational absorption coefficient for all single vibrational transitions with a change in v of $+1$. The effect of stimulated emission is included. Temperature is given in thousands of degrees Kelvin. The attenuation of a monochromatic light beam may be calculated from $I/I_0 = \exp(-A_{\tilde{\nu}} \rho^2 L)$, where ρ is dimensionless H_2 density (see eq. 43).

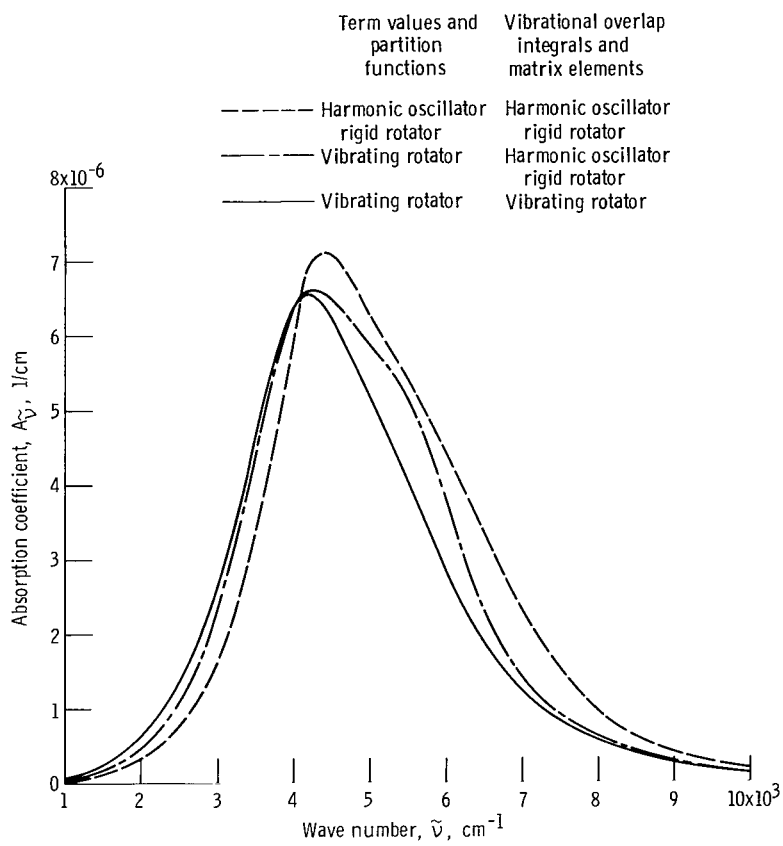


Figure 14. - Pressure-induced vibrational absorption coefficient calculated using three models. Temperature is 4000 K. All single vibrational transitions with a change in v of +1 were included.

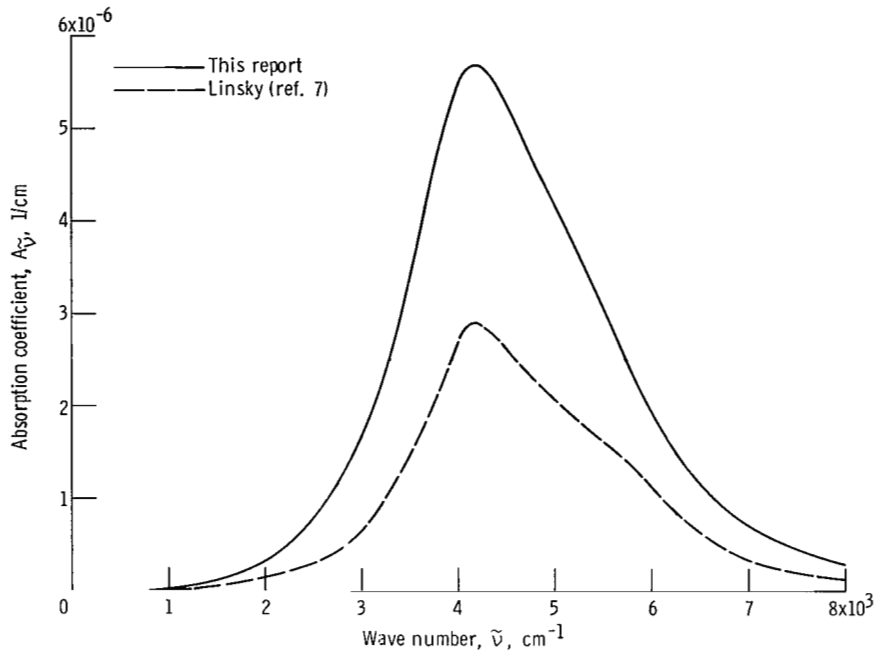


Figure 15. - Comparison of pressure-induced vibrational absorption coefficient in the fundamental region according to two different theories. The temperature is 3000 K.

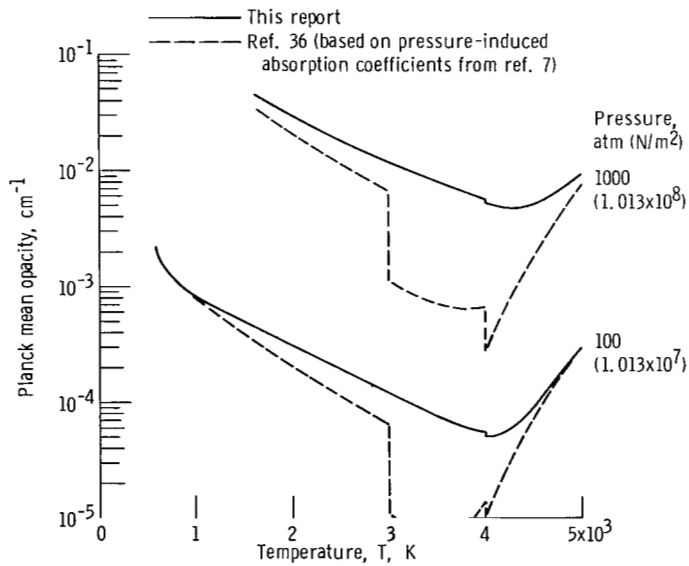


Figure 16. - Effect of $H_2 - H_2$ pressure-induced vibrational absorption coefficients of this report on the Planck mean opacity of hydrogen. The discontinuities in the dashed curves at 3000 K are due to reference 7 giving no vibrational absorption coefficients above 3000 K. The discontinuities in all curves at 4000 K are due to reference 7 giving no rotational absorption coefficients above 4000 K.

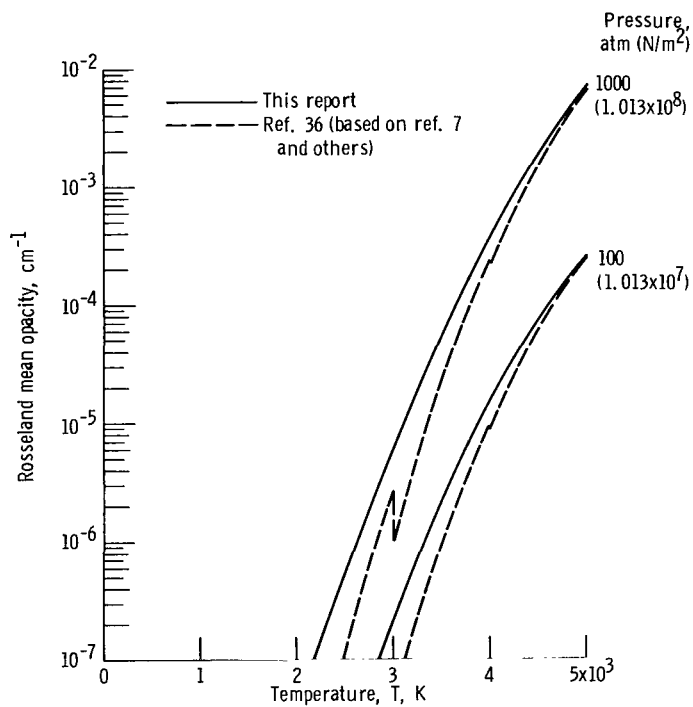


Figure 17. - Effect of H₂ - H₂ pressure-induced vibrational absorption coefficients of this report on the Rosseland mean opacity of hydrogen. Discontinuities in dashed curves at 3000 and 4000 K result from reference 7 giving no vibrational and rotational absorption coefficients, respectively, above these temperatures.